

# Human4DiT: Free-view Human Video Generation with 4D Diffusion Transformer

Ruizhi Shao<sup>1,\*</sup>, Youxin Pang<sup>1,\*</sup>, Zerong Zheng<sup>2</sup>, Jingxiang Sun<sup>1</sup>, Yebin Liu<sup>1</sup>  
<sup>1</sup>Department of Automation, Tsinghua University <sup>2</sup>NNKosmos Technology



Figure 1. We propose **Human4DiT**, a novel approach to generate high-quality, spatio-temporally coherent human videos given a reference image. With the proposed 4D diffusion transformer, our method is capable of generating monocular video, multi-view video, 3D static video, and free-view video.

## Abstract

We present a novel approach for generating high-quality, spatio-temporally coherent human videos from a single image under arbitrary viewpoints. Our framework combines the strengths of U-Nets for accurate condition injection and diffusion transformers for capturing global correlations across viewpoints and time. The core is a cascaded 4D transformer architecture that factorizes attention across views, time, and spatial dimensions, enabling efficient modeling of the 4D space. Precise conditioning is achieved by injecting human identity, camera parameters, and temporal signals into the respective transformers. To train this model, we curate a multi-dimensional dataset spanning images, videos, multi-view data and 3D/4D scans, along with a multi-dimensional training strategy. Our approach overcomes the limitations of previous methods based on GAN or UNet-based diffusion models, which struggle with complex motions and viewpoint changes. Through extensive experiments, we demonstrate our method’s ability to synthesize realistic, coherent and free-view human videos, paving the way for advanced multimedia applications in areas such as virtual reality and animation. Our project website is <https://human4dit.github.io>.

## 1. Introduction

Human video generation is an active topic in the field of video generation. It has widespread applications in areas such as virtual reality, animation, gaming, and movie production. Moreover, generating realistic human videos holds great significance for advancing multimedia technologies and enabling new forms of human-computer interaction.

Recently, with the rapid development of diffusion models, especially latent diffusion models [24], leveraging diffusion models for human video generation has become the mainstream approach [7, 37, 41, 50]. To incorporate human priors as control conditions into the diffusion model, some approaches [11] have adopted skeleton-based schemes, using the skeletal connectivity graph as a control condition either through ControlNet [47] or by concatenating it with the input. Other methods are based on the SMPL body model template [16], injecting SMPL-derived representations such as UV maps, depth, normals [50], or direct dense pose embeddings [41] into the diffusion model. Current human video diffusion models based on the UNet architecture [25] from Stable Diffusion could inject control conditions into the network in a pixel-aligned manner. However, the UNet’s reliance on local convolutional operations makes it more focus on local generation, resulting in relatively poorer performance for the global aspects, especially when generating long and complex human motions. Moreover, these

\* Equal Contribution.

methods only consider the human body itself, neglecting viewpoint information from the camera perspective, especially for scenarios involving significant viewpoint changes such as 360-degree free-viewpoint human video generation. Incorporating viewpoint control signals into the network while simultaneously maintaining coherence across different viewpoints and time poses a significant challenge.

To overcome the challenges of generating complex human motions across views and time, we propose a novel video generation network architecture that combines the strengths of UNets and diffusion transformers. The UNet component is responsible for accurate pixel-aligned condition injection, which has been proven powerful for human image generation. However, it remains a challenge to ensure temporal consistency when using UNet-like architectures to generate long videos. Recently, OpenAI’s recent work on long video generation, SORA [20], adopted a diffusion transformer [21] architecture and demonstrated substantially better realism and spatio-temporal coherence than UNet-based competitors. Inspired by SORA, we introduce a 4D diffusion transformer, which learns global correlations of complex human motions across views and time, thereby preserving spatio-temporal consistency of generated human videos. In practice, we first apply UNet to extract pixel-aligned features, after which these features are tokenized and processed by the 4D diffusion transformer with self-attention mechanisms.

However, directly applying a diffusion transformer to learn correlations over the views and time would be computationally prohibitive. Therefore, we propose an efficient novel 4D transformer architecture. Its core principle is to cascadingly learn the correlations across the 4D space (view, time, height, width) via self-attention. Specifically, we factorize the 4D diffusion transformer into three transformer blocks: 2D image transformer blocks, temporal transformer blocks, and view transformer blocks, each attending to different dimensions of the 4D space. These three types of blocks are interconnected to form a 4D transformer block. Multiple such 4D transformer blocks are then cascaded to construct the final 4D transformer. This efficiently captures the interrelations between body parts (height, width) across viewpoints (views) and time steps (times).

Based on our proposed network architecture, we incorporate different control signals into the respective network modules for precise control, including SMPL, human identity, time, and camera parameters. SMPL features and human identity embeddings are extracted by the guidance UNet and injected into all three transformers; view embeddings are encoded from camera parameters and injected into the view transformer; temporal embeddings are injected into the temporal transformer. Through these modules, we effectively inject various control conditions into the net-

work, enabling arbitrary viewpoint control and the generation of high-quality, coherent human videos.

To train our proposed 4D diffusion transformer model, we also collected a large multi-dimensional dataset and devised a multi-dimensional training strategy that fully leverages all available data modalities. Our multi-dimensional dataset comprises images, videos, multi-view videos, 3D scans, as well as a limited amount of 4D scans spanning different viewpoints and time steps. During the inference stage, we propose a spatio-temporally consistent diffusion sampling strategy that enables the generation of long free-viewpoint 360-degree videos despite limited spatio-temporal window constraints. The strategy is carried out with two stages. The first stage treats the free-view video as a monocular long video sequence, maximizing the temporal window to ensure long-term temporal consistency. After that, the second stage regards the free-view video as a collection of multi-view video clips, using a larger viewpoint window with a smaller temporal window, encouraging consistency across viewpoints.

To summarize, our main contributions are threefold:

- We are the first to introduce diffusion transformers to human video generation. Combined with methods that simply use UNet and several control modules, our method achieves higher-quality free-viewpoint and spatio-temporally consistent generation of long human videos.
- We propose an efficient 4D diffusion transformer architecture composed of three transformers attending to 2D images, time, and viewpoints respectively, significantly reducing computational requirements while effectively capturing correlations between body parts across space and time.
- We collect a large multi-dimensional 4D human dataset and introduce a multi-dimensional training strategy that fully leverages data from all modalities.
- During inference, we also propose a spatio-temporally consistent diffusion sampling strategy to generate coherent 360-degree long human videos.

## 2. Related Work

### 2.1. Human Video Generation

Human video generation is the task of creating realistic and temporally coherent videos of humans from input data such as text descriptions, images, or motion sequences. The current paradigm of human video generation lies in two main categories: GAN-based and diffusion-based approaches.

GAN-based methods [28–30, 32, 38, 39] leverage the inherent generative capabilities of adversarial networks [5, 19] to spatially transform reference images according to input motion. These approaches commonly employ warping functions to generate sequential video frames, aiming to fill

in missing regions and improve visually implausible areas within the generated content. While GAN-based methods have shown promising results in dynamic visual content generation, they often struggle with effectively transferring motion, especially when there are significant variations in human identity and scene dynamics between the reference image and the source video motion. This can lead to unrealistic visual artifacts and temporal inconsistencies in the synthesized videos.

On the other hand, diffusion models, known for the superior generation quality and stable controllability, have been successfully integrated into human image animation. These models [2, 7, 10, 37, 41, 50] employ various strategies, such as texture diffusion blocks, optical flow synthesis in latent space, and motion representation using flow maps, to enhance the visual fidelity of the generated videos. Animate Anyone [7] employs a UNet-based ReferenceNet to extract features from reference images and incorporates pose information through an efficient pose guider. However, recent diffusion-based methods are still mainly relying on image diffusion model and face challenges in maintaining texture consistency and temporal stability across frames. Furthermore, these methods don't explore view controllability.

## 2.2. Diffusion Model with Camera Control

Camera information is conditioned in diffusion models for view control. One line of works inject camera parameters into the text-to-image diffusion models for consistent view synthesis from a single input image, which has inspired researchers to explore their potential for generating consistent multi-view images. Zero-1-to-3 [13] finetunes Stable diffusion by conditioning camera poses for zero-shot novel view synthesis. Syncdreamer [14] employs 3D volumes and depth-wise attention to maintain consistency across views. MVDream [27] and other methods like Wonder3D [15] and Zero123++ [26] leverage 3D self-attention to extend multi-view image generation to more general and efficient. There are other works [6, 42] inject camera information into text-to-video (T2V) models. For example, Direct-a-Video [42] injects quantitative camera movements into temporal cross-attention blocks for view control.

## 2.3. Diffusion Transformer

The transformer architecture [36] has revolutionized the field of natural language processing, with models like GPT [22, 23] achieving remarkable success. Recent research has demonstrated the potential of transformers in various computer vision tasks, including image classification [33, 45], semantic segmentation [31, 40, 49].

Building upon this progress, the Diffusion Transformer (DiT) [21] and its variants [1, 48] have taken a step further by substituting the conventional convolutional-based U-Net backbone [25] with transformers in diffusion models. This

architectural shift offers enhanced scalability compared to U-Net-based models, enabling the seamless expansion of model parameters. Recently, the transformer architecture is also integrated into text-to-video models [17, 18, 20], improving generation performance.

## 3. Overview

Given a reference image of a person  $\mathbf{y}_r$ , a sequence of dynamic SMPL models  $\{\mathbf{P}_{i=1}^T = (\theta, \beta)_{i=1}^T\}$ , and camera parameters  $\{\mathbf{c}_{i=1}^V\}$ , the goal of our method is to generate a video of that person performing the corresponding motion from the specified viewpoint. The overall pipeline of our approach is illustrated in Figure 2. Since our framework is based on a latent diffusion transformer, we first generate a noisy latent representation  $\mathbf{x}_t$ . We then inject  $\mathbf{y}_r$ ,  $\{\mathbf{P}_{i=1}^T\}$ , and  $\{\mathbf{c}_{i=1}^V\}$  as control signals into the diffusion transformer, which iteratively performs denoising to ultimately generate the latent video  $\mathbf{x}_0$  (Sec. 4).

To train our proposed model, we collected a multi-dimensional human dataset comprising images, videos, multi-view data, as well as 3D and 4D human data. We further introduce a multi-dimensional mixed training strategy that fully leverages all available data modalities for effective network training (Sec. 5).

During the inference stage, to enable the generation of free-viewpoint long-duration human motion videos under limited temporal and viewpoint window constraints, we propose an efficient diffusion sampling strategy. This strategy achieves improved spatio-temporal coherence by planning viewpoint and temporal window sizes of different scales in the diffusion sampling process (Sec. 6).

## 4. Network Structure

In this section, we introduce the core components of our network structure: the 4D diffusion transformer and the control condition injection modules. To efficiently establish spatio-temporal relationships, our 4D diffusion transformer adopts a cascaded structure consisting of the 2D image, the temporal, and the view transformer blocks. Additionally, our control condition injection modules comprise the reference image injection module, the SMPL injection module, the time injection module, and the viewpoint injection module. Notably, the reference image injection module and the SMPL injection module utilize UNet architectures to ensure pixel-aligned injection of the control conditions.

### 4.1. 4D Diffusion Transformer

Our 4D diffusion transformer performs denoising on a randomly initialized noisy multi-view latent human video  $\mathbf{x}_t$ . After multiple denoising steps, it produces the denoised output  $\mathbf{x}_0$ , which is eventually decoded by a VAE to generate the video. The input  $\mathbf{x}_t$  could be regarded as a set of to-

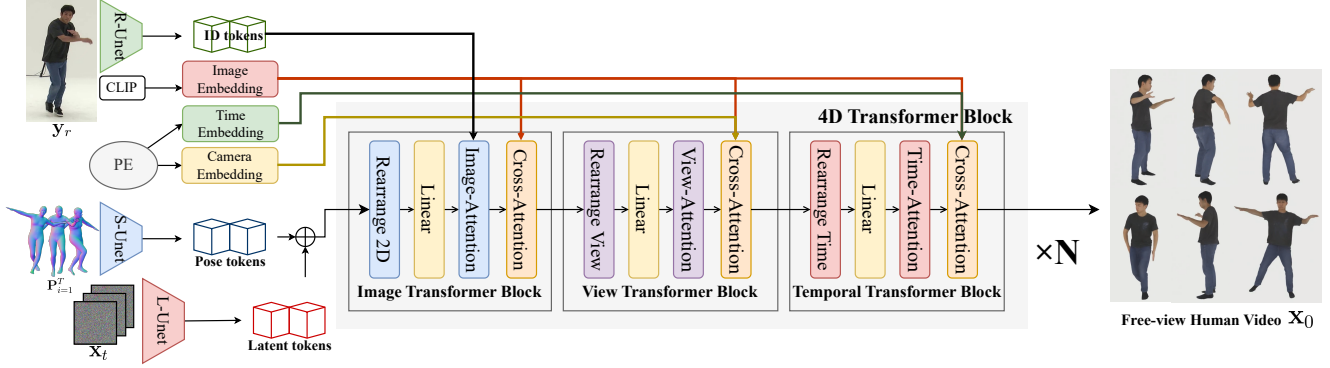


Figure 2. **Pipeline of Human4DiT**: our framework is based on 4D diffusion transformer, which adopts a cascaded structure consisting of the 2D image, the view transformer, and the temporal blocks. The input contains a reference image  $y_r$ , dynamic SMPL sequences  $\mathbf{P}$ , and camera parameters  $\mathbf{c}$ . Starting from a generated noisy latent representation  $x_t$ , we then denoise  $x_t$  conditioned on  $y_r$ ,  $\mathbf{P}$ , and  $\mathbf{c}$ . Firstly, the 2D image transformer block is designed to capture spatial self-attention within each frame. In addition,  $y_{i,d}$  extracted from  $y_r$  is also injected to ensure identity consistency. Secondly, we use the view transformer block to learn correspondences across different viewpoints conditioned on  $\mathbf{c}$ . Finally, we adopt a temporal transformer to capture temporal correlations with time embedding. The human image embedding  $y_e$  extracted through CLIP is shared by three blocks.

kens in 5D ( $\mathbf{x}_t \in \mathbb{R}^{V \times T \times H \times W \times C}$ ), where  $C$  represents the feature dimension of each token,  $V$  is the viewpoint dimension,  $T$  is the time dimension, and  $H$  and  $W$  are the height and width, respectively. Our 4D diffusion transformer incorporates three types of transformer blocks to efficiently establish correlations across viewpoints, time, and 2D spatial dimensions.

First, we feed  $x_t$  into a 2D image transformer block to capture spatial self-attention within each frame:

$$\begin{aligned} \mathbf{x}_t^s &= \text{rearrange}(\mathbf{x}_t, (V \times T, H \times W, C)), \\ \mathbf{Q}_s, \mathbf{K}_s, \mathbf{V}_s &= f_s^{\mathbf{Q}}(\mathbf{x}_t^s), f_s^{\mathbf{K}}(\mathbf{x}_t^s), f_s^{\mathbf{V}}(\mathbf{x}_t^s), \\ \hat{\mathbf{x}}_t^s &= \text{softmax}\left(\frac{\mathbf{Q}_s \mathbf{K}_s^T}{\sqrt{d_k}}\right) \mathbf{V}_s, \end{aligned} \quad (1)$$

where  $f_s^{\mathbf{Q}}, f_s^{\mathbf{K}}, f_s^{\mathbf{V}}$  are the linear layers in the transformer block. The rearrange operation reshapes the tensor  $\mathbf{x}_t$  into a 3D tensor  $\mathbf{x}_t^s \in \mathbb{R}^{(V \times T) \times (H \times W) \times C}$ , where the first dimension  $V \times T$  is treated as the batch size. The actual attention operation is then performed on the last two dimensions  $H \times W$  and  $C$ , which correspond to the 2D spatial dimensions of the images. After 2D image transformer, we further model correspondences across different viewpoints through the view transformer block:

$$\begin{aligned} \mathbf{x}_t^v &= \text{rearrange}(\hat{\mathbf{x}}_t^s, (T, V \times H \times W, C)), \\ \mathbf{Q}_v, \mathbf{K}_v, \mathbf{V}_v &= f_v^{\mathbf{Q}}(\mathbf{x}_t^v), f_v^{\mathbf{K}}(\mathbf{x}_t^v), f_v^{\mathbf{V}}(\mathbf{x}_t^v), \\ \hat{\mathbf{x}}_t^v &= \text{softmax}\left(\frac{\mathbf{Q}_v \mathbf{K}_v^T}{\sqrt{d_k}}\right) \mathbf{V}_v, \end{aligned} \quad (2)$$

In the view transformer, due to the substantial variations across different viewpoints, especially between frontal,

side, and back views, we perform attention jointly across the viewpoint and the 2D spatial dimensions. This attention allows for better modeling of the global correlations across the entire frame. It also makes the view transformer the most computationally and memory intensive component, limiting the maximum viewpoint window size. We will address this constraint during the inference process, as discussed later. After the view transformer, we finally employ a temporal transformer to capture temporal correlations across time steps.

$$\begin{aligned} \mathbf{x}_t^m &= \text{rearrange}(\hat{\mathbf{x}}_t^v, (V \times H \times W, T, C)), \\ \mathbf{Q}_m, \mathbf{K}_m, \mathbf{V}_m &= f_m^{\mathbf{Q}}(\mathbf{x}_t^m), f_m^{\mathbf{K}}(\mathbf{x}_t^m), f_m^{\mathbf{V}}(\mathbf{x}_t^m), \\ \hat{\mathbf{x}}_t^m &= \text{softmax}\left(\frac{\mathbf{Q}_m \mathbf{K}_m^T}{\sqrt{d_k}}\right) \mathbf{V}_m, \end{aligned} \quad (3)$$

The three transformer blocks (2D image, view, and temporal) are interconnected to form a single 4D transformer block. Our complete 4D diffusion transformer architecture is composed of multiple cascaded 4D transformer blocks. Through this cascaded multi-level attention scheme, our approach significantly reduces the computational overhead while improving the training efficiency and effectively ensuring spatio-temporal consistency in the generation process.

## 4.2. Control Modules

### 4.2.1 Camera Control Module

To incorporate camera viewpoint control into the network, we assume the first camera  $\mathbf{c}_1$  as the world coordinate sys-

Dataset	Clips	Frames	Views	Resolution	3D	Dynamic	SMPL	Body
HumanArt [9]	-	50k	1	512 <sup>2</sup> -1024 <sup>2</sup>	✗	✗	Ground Truth	Half-body + Full-body
TikTok [8]	2k	600k	1	480P-720P	✗	✓	Fitting	Half-body + Full-body
TalkShow [43]	1k	300k	1	480P-720P	✗	✓	Fitting	Half-body
AIST [34]	10k	2000k	6	1080P	✗	✓	Ground Truth	Full-body
Motion-X [12]	10k	1000k	1	720P-1080P	✗	✓	Ground Truth	Full-body
DNA-rendering [4]	2k	400k	16	4K	✗	✓	Fitting	Full-body
Twindom [35]	2k	360k	180	1024 <sup>2</sup>	✗	✓	Fitting	Full-body
THuman2.0 [44]	500	90k	180	1024 <sup>2</sup>	✓	✗	Ground Truth	Full-body
THuman-CloSET [46]	500	90k	180	1024 <sup>2</sup>	✓	✗	Ground Truth	Full-body
Bedlam [3]	10k	1500k	1	720P-1080P	✗	✓	Ground Truth	Full-body
<b>Human4DiT-3D</b>	5k	900k	180	1024 <sup>2</sup>	✓	✗	Fitting	Full-body
<b>Human4DiT-Video</b>	10k	2000k	1	720P-1080P	✗	✓	Fitting	Full-body
<b>Human4DiT-4D</b>	100	168k	180	1024 <sup>2</sup>	✓	✓	Fitting	Full-body

Table 1. The collected multi-dimensional training dataset.

tem, extract its rotation matrix (i.e., the identity matrix) as a 9D tensor  $\mathbf{r}_1$ , and apply positional encoding:

$$\mathbf{y}_c = (\sin(2^0\pi\mathbf{r}_1), \cos(2^0\pi\mathbf{r}_1), \dots, \sin(2^{L-1}\pi\mathbf{r}_1), \cos(2^{L-1}\pi\mathbf{r}_1)) \quad (4)$$

The parameters of other cameras  $\{\mathbf{c}_{i=2}^V\}$  are computed as rotation matrices relative to the first camera, and their encodings are obtained through the same positional encoding process. We then map these encodings to the same dimension as the CLIP image embeddings using an MLP  $f_c$  and inject them into the view transformer module via addition to influence the intermediate features after self-attention:

$$\mathbf{x}_t^{v'} = \mathbf{x}_t^v + f_c(\mathbf{y}_c) \quad (5)$$

This relative encoding formulation effectively represents the correlations between different viewpoints, enabling better generation with varying multi-view setups.

#### 4.2.2 Temporal Embedding Module

To incorporate temporal control into the network, we apply positional encoding directly to the time  $T_m$  (frame number):

$$\mathbf{y}_m = (\sin(2^0\pi T_m), \cos(2^0\pi T_m), \dots, \sin(2^{L-1}\pi T_m), \cos(2^{L-1}\pi T_m)) \quad (6)$$

We then map the temporal encoding to the latent space using an MLP  $f_m$  and add it to the temporal transformer’s features after self-attention:

$$\mathbf{x}_t^{m'} = \mathbf{x}_t^m + f_m(\mathbf{y}_m) \quad (7)$$

#### 4.2.3 SMPL Control Module

To inject the SMPL parameters into the network, we first obtain the SMPL mesh vertex positions from the given

shape and pose parameters  $\mathbf{p}_i = LBS(\theta_i, \beta_i)$  of each frame  $i$ . We then render these vertices  $\mathbf{p}_i$  into normal maps  $\mathbf{M}_n(i, v)$  using camera parameters  $\mathbf{c}_v$ , as normals provide an effective representation of the 3D human. Since the camera parameters  $\mathbf{c}_v$  have already been injected into the network, we decouple the SMPL information from the rendered normal maps by multiplying it with the inverse of the camera rotation matrix  $\mathbf{r}_v^{-1}$ . We then use a UNet  $E_p$  to extract features  $\mathbf{y}_n$  from these SMPL rendered normal maps  $\mathbf{M}_n(i, v)$ . These features  $\mathbf{y}_n$  are eventually added to the input  $\mathbf{x}_t$  of the 4D Diffusion Transformer before being fed into the network. Through this approach, the control condition is injected into the network in a pixel-aligned manner, ensuring consistent and accurate human motion video generation.

#### 4.2.4 Human Identity Reference Module

During human video generation, we extract the human identity from a reference image and inject it into the network. We employ two ways to maintain identity consistency. First, similar to the SMPL injection, we use a UNet  $E_{id}$  to extract human features  $\mathbf{y}_{id}$  from the reference image. These features are then added to the input of the 4D diffusion transformer  $\mathbf{x}_t$ , allowing the network to better capture the detailed identity characteristics from the reference image. Additionally, we extract an image embedding  $\mathbf{y}_e$  using CLIP and inject it into each transformer block via cross-attention after the self-attention mechanism:

$$\mathbf{Q}, \mathbf{K}, \mathbf{V} = f^{\mathbf{Q}}(\tilde{\mathbf{x}}_t), f^{\mathbf{K}}(\mathbf{y}_e), f^{\mathbf{V}}(\mathbf{y}_e), \quad (8)$$

$$\tilde{\mathbf{x}}_t = \text{softmax}\left(\frac{\mathbf{Q}\mathbf{K}^T}{\sqrt{d_k}}\right)\mathbf{V}$$

This ensures that the generated output maintains global consistency with the reference human identity in addition to preserving local details.

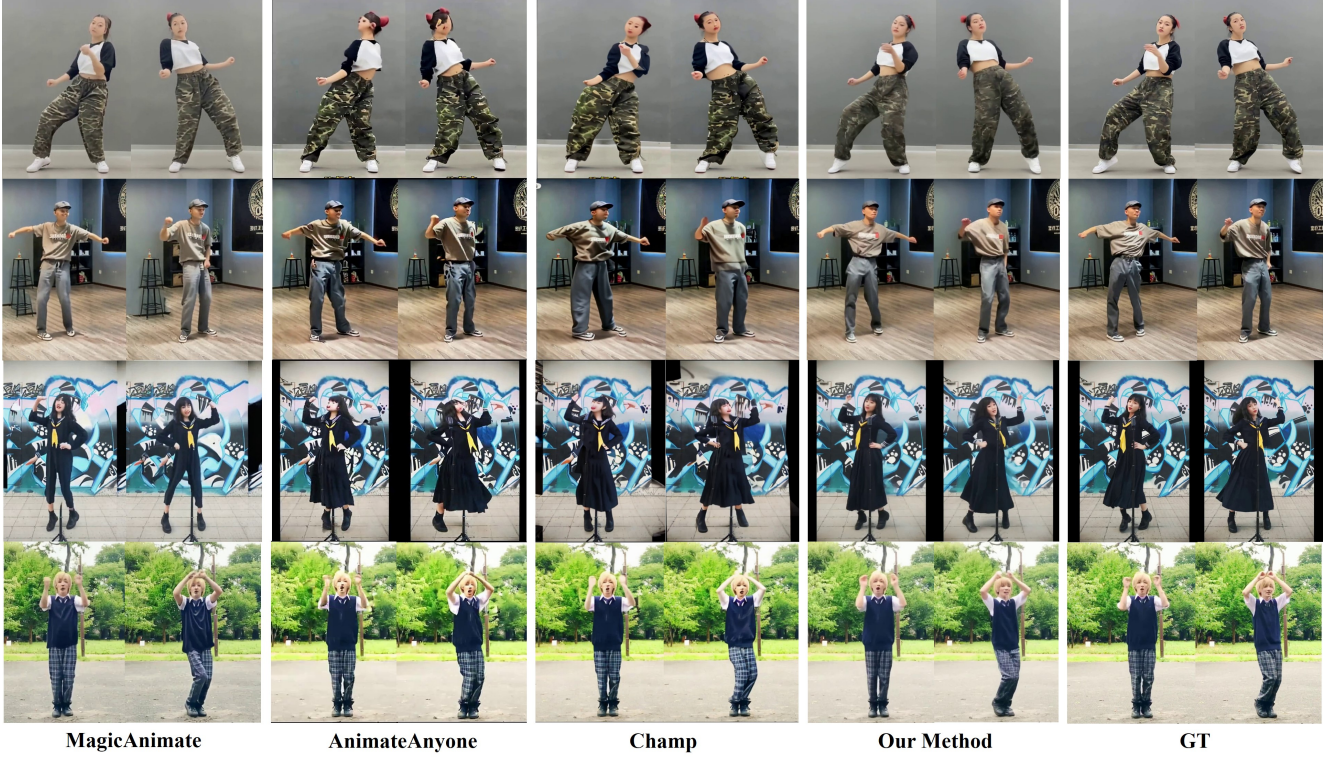


Figure 3. Qualitative comparison on monocular video.

## 5. Dataset and Training Strategy

To train this 4D transformer model, we collected a multi-dimensional dataset and devised a multi-dimensional training strategy that fully leverages all available data modalities. As shown in Tab. 1, our multi-dimensional dataset comprises human images, videos, multi-view videos, 3D data, as well as a small amount of 4D data spanning different viewpoints and time steps.

We employ different training strategies for each data modality. For the 2D images dataset, we only train the 2D transformer, using the CLIP image embedding as the human identity condition. For the single-view video dataset, we train the 2D and temporal transformers, randomly selecting one frame from the video as the reference image. For multi-view videos, we train all transformers simultaneously, randomly choosing one frame from the multi-view data as the reference image. For 3D dataset, we train our transformer with two strategies. multi-view images and train only the 2D and view transformers, randomly selecting one rendered view as the reference. For 4D dataset, we render it into dense-view videos or videos with continuous viewpoint movements and train all transformers concurrently.

This multi-dimensional training approach allows us to effectively leverage diverse data sources, with each modality contributing to different components of the model. The

unified 4D transformer architecture seamlessly integrates information from all modalities during training, enabling coherent free-viewpoint human video generation.

---

### Algorithm 1: Efficient Spatial-Temporal Sampling

---

**Input:**  $T_i$  (number of inference timesteps);  $\mathbf{y}$  (Control signals);  $T_L$  (number of frames);  $M_T^1, M_T^2, M_V^2$  (window size of view and time);  $\epsilon_\theta$  (4D diffusion transformer)

**Output:**  $x_0$  (sampled latent video)

- 1  $\mathbf{x}_t \sim \mathcal{N}(0, I), \epsilon \sim \mathcal{N}(0, I)$ ;
  - 2  $N_T^1 = \frac{T_L}{M_T^1}, N_T^2 = \frac{T_L}{M_T^2}, N_V^2 = \frac{T_L}{M_V^2}$ ;
  - 3 **for**  $t \leftarrow T_i$  **to** 1 **do**
  - 4     **for**  $m \leftarrow 1$  **to**  $N_T^1$  **do**
  - 5          $\text{slice}^1 = [mM_T^1 : (m+1)M_T^1]$ ;
  - 6          $\epsilon^1[\text{slice}^1] = \epsilon_\theta(\mathbf{x}_t[\text{slice}^1], t, \mathbf{y}[\text{slice}^1])$ ;
  - 7     **for**  $m \leftarrow 1$  **to**  $N_T^2, v \leftarrow 1$  **to**  $N_V^2$  **do**
  - 8          $\text{slice}^2 = [v : T_L : N_V^2, mM_T^2 : (m+1)M_T^2]$ ;
  - 9          $\epsilon^2[\text{slice}^2] = \epsilon_\theta(\mathbf{x}_t[\text{slice}^2], t, \mathbf{y}[\text{slice}^2])$ ;
  - 10      $\mu_\theta \leftarrow \frac{1}{\sqrt{\alpha_t}} \left( x_t - \frac{\beta_t}{\sqrt{1-\alpha_t}} (\lambda_1 \epsilon_1 + \lambda_2 \epsilon_2) \right)$ ;
  - 11      $x_{t-1} \leftarrow \mu_\theta + \sigma_t \epsilon$
  - 12 **return**  $x_0$ ;
-

Method	PSNR $\uparrow$	SSIM $\uparrow$	LPIPS $\downarrow$	FVD $\downarrow$
Disco	20.07	0.661	0.285	585.3
MagicAnimate	21.08	0.717	0.256	550.7
AnimateAnyone	22.18	0.789	0.195	479.5
Champ	22.88	0.824	0.171	359.3
Ours	<b>26.12</b>	<b>0.888</b>	<b>0.116</b>	<b>237.4</b>

Table 2. Quantitative comparison on monocular video.

## 6. Efficient Spatial-Temporal Sampling

Our 4D diffusion transformer is capable of generating multi-view human motion videos. However, it cannot directly generate free-viewpoint videos where both viewpoint and time vary simultaneously. This limitation arises from computational memory constraints, where the total number of frames  $M$  in the network input is bounded by the product of the temporal window size  $M_T$  and the view window size  $M_V$ . To enable generation of long free-view videos, we propose an efficient and spatio-temporally consistent sampling method. During the denoising process, this method employs two strategies. The first strategy treats the free-view video as a monocular long video sequence, maximizing the temporal window  $M_T^1$  to ensure long-term temporal consistency. The second strategy regards the free-view video as a collection of multi-view short video clips, using a larger viewpoint window  $M_V^2$  with a smaller temporal window  $M_T^2$ , focusing on maintaining consistency across viewpoints. During denoising, the noise predictions from these two strategies are combined using respective weightings  $\lambda_1, \lambda_2$ . The specific sampling algorithm is outlined in Alg. 1.

This sampling approach combines the advantages of both strategies. Globally, it leverages the view transformer to maintain consistency across large viewpoint separations. For smaller inter-frame motions between adjacent viewpoints, the temporal transformer ensures coherence. Ultimately, this method achieves spatio-temporally consistent generation of long free-viewpoint human motion videos under limited input window constraints.

## 7. Experiment

In this section, to validate the capabilities of our 4D diffusion transformer, we conducted comprehensive comparisons against current state-of-the-art human video generation methods including Disco [37], MagicAnimate [41], AnimateAnyone [7], and Champ [50] on monocular video, multi-view video, 3D static video, and free-view video generation.

### 7.1. Implementation Details

Our method is based on the latent diffusion model that utilizes the VAE from Stable Diffusion XL. Our 4D diffusion

Method	PSNR $\uparrow$	SSIM $\uparrow$	LPIPS $\downarrow$	FVD $\downarrow$
Disco	18.86	0.796	0.293	646.2
MagicAnimate	19.30	0.845	0.232	517.3
AnimateAnyone	19.87	0.858	0.216	472.8
Champ	20.15	0.886	0.203	442.4
Ours (temporal)	21.16	0.907	0.190	374.2
Ours	<b>22.40</b>	<b>0.920</b>	<b>0.159</b>	<b>296.53</b>

Table 3. Quantitative comparison on multi-view video.

Method	PSNR $\uparrow$	SSIM $\uparrow$	LPIPS $\downarrow$	FVD $\downarrow$
Disco	17.13	0.882	0.209	451.6
MagicAnimate	19.28	0.906	0.159	356.4
AnimateAnyone	20.53	0.922	0.111	285.4
Champ	21.11	0.927	0.106	204.3
Ours (temporal)	22.58	0.941	0.058	165.2
Ours	<b>23.37</b>	<b>0.962</b>	<b>0.045</b>	<b>110.0</b>

Table 4. Quantitative comparison on 3D static video.

Method	PSNR $\uparrow$	SSIM $\uparrow$	LPIPS $\downarrow$	FVD $\downarrow$
Disco	19.98	0.872	0.169	559.7
MagicAnimate	21.74	0.920	0.135	418.4
AnimateAnyone	22.01	0.912	0.131	410.3
Champ	23.35	0.922	0.110	347.6
Ours (temporal)	24.74	0.936	0.085	274.1
Ours	<b>25.02</b>	<b>0.947</b>	<b>0.062</b>	<b>234.8</b>

Table 5. Quantitative comparison on Free-view video.

transformer contains 10 4D transformer blocks, totaling 30 transformer layers. Our U-Net compresses the input by a factor of 8, with each token having 1280 channels, and the text embedding and image identity embedding are also mapped to 1280 channels. During training, the video data is resized to 768x768 resolution, and for each GPU, the input consists of 24 frames. When training on image data, we use a batch size of 24, while for monocular video training, we use a batch size of 1 with a video length of 24. For multi-view video, 3D video, and free-view video training, we use a batch size of 1 with a video length of 6 and 4 views. We employed 24 A100 GPUs, and the total training time was 14 days.

### 7.2. Comparisons

**Comparisons on Monocular Video.** For monocular video, we randomly select 200 videos from the DiffuHuman-video dataset as our test set for comparison, with the first frame of each video serving as the reference image. During inference, our method employs a temporal window of 24 frames, with an overlap of 6 frames between consecutive windows. For Disco [37], MagicAnimate [41], and Champ [50], we use their official open-source code. As for AnimateAnyone [7], we employ the opensource implementation from

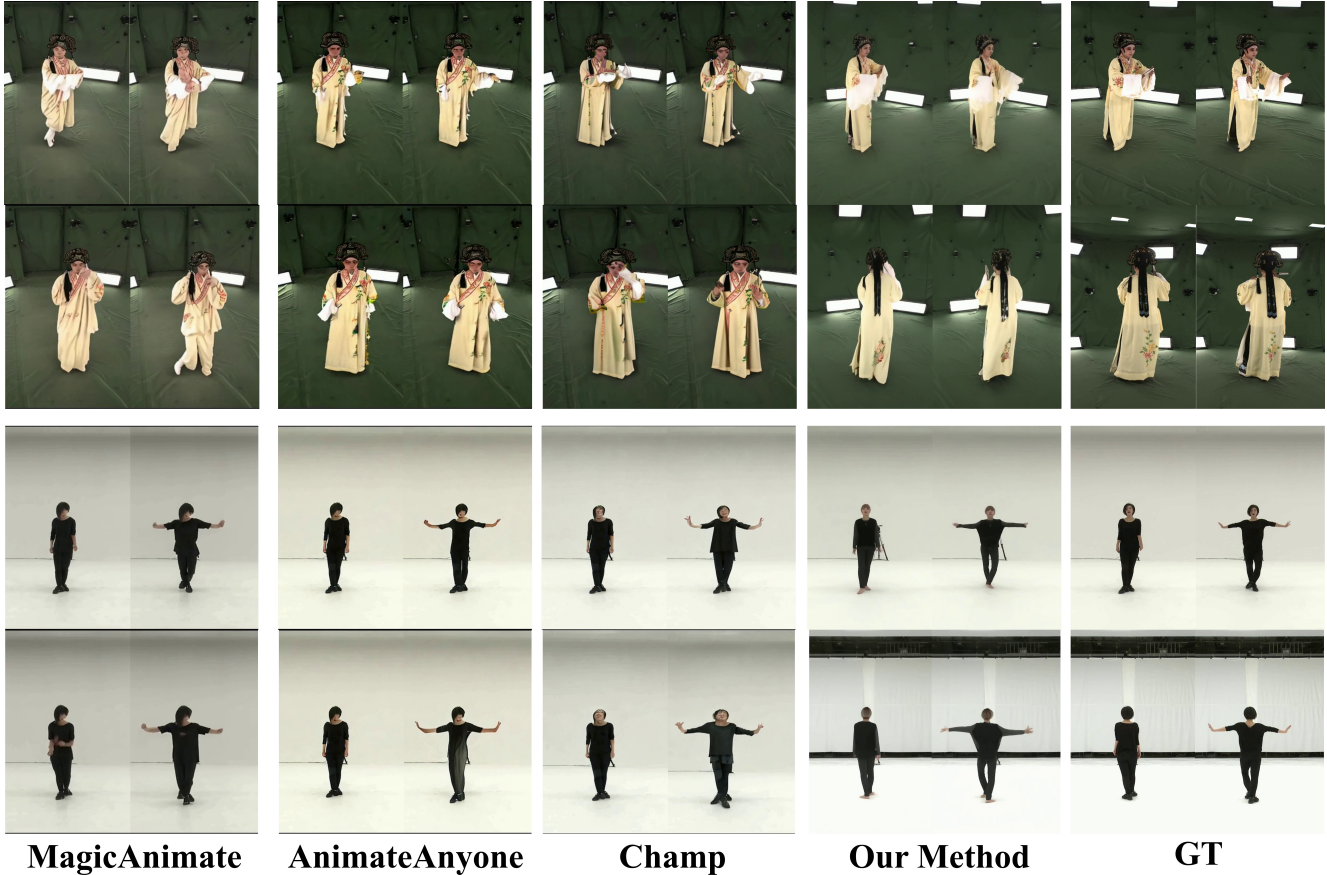


Figure 4. Qualitative comparison multi-view video.

MooreThreads . Quantitative comparisons are presented in Tab. 2, where our method demonstrates a clear numerical advantage, significantly outperforming other approaches. This highlights the superiority of our 4D diffusion transformer over U-Net-based methods. We have also conducted qualitative comparisons, with results shown in Fig. 3. Our method generates more natural dynamic effects with fewer deformation and jitter artifacts compared to other methods, indicating the 4D transformer’s stronger capability in establishing spatio-temporal consistency than U-Net-based approaches. Please refer to our submitted project webpage for dynamic video effects.

**Comparisons on Multi-view Video.** For multi-view settings, we select 25 multi-view groups from the AIST and DNA-rendering datasets respectively as our test set for comparison, with each group containing videos captured from 4 different viewpoints. We use the first frame of the frontal view as the reference image. During inference, our method employs the spatial-temporal sampling strategy, with a spatial window size of 4 views and a tempo-

ral window of 6 frames for spatial sampling. For temporal sampling, the window size is 24 frames. The blending weights for spatial and temporal  $\lambda_1, \lambda_2$  are set to 0.5 and 0.5, respectively. For Disco, MagicAnimate, Champ, and AnimateAnyone, we treat each view’s video as a monocular video and perform inference separately. Quantitative comparisons are presented in Tab. 3, where we masked out the backgrounds for metric computation since inferring other views’ backgrounds from a single view is an ill-posed problem. Our method outperforms others, demonstrating the 4D diffusion transformer’s superior ability to establish stronger cross-view correlations compared to U-Net-based approaches. We have also conducted qualitative comparisons, with results shown in Fig. 4. Our method generates spatio-temporally consistent multi-view videos without exhibiting multi-face artifacts. Please refer to the project webpage for dynamic video effects.

**Comparisons on 3D Static Video.** For 3D setting, we select 100 3D scans from THuman2.0 and render them into 3D static videos as our test set for comparison. We use the frontal view as the reference image. During inference, our method employs the same spatial-temporal sampling strat-





Figure 5. Qualitative comparison 3D static video.

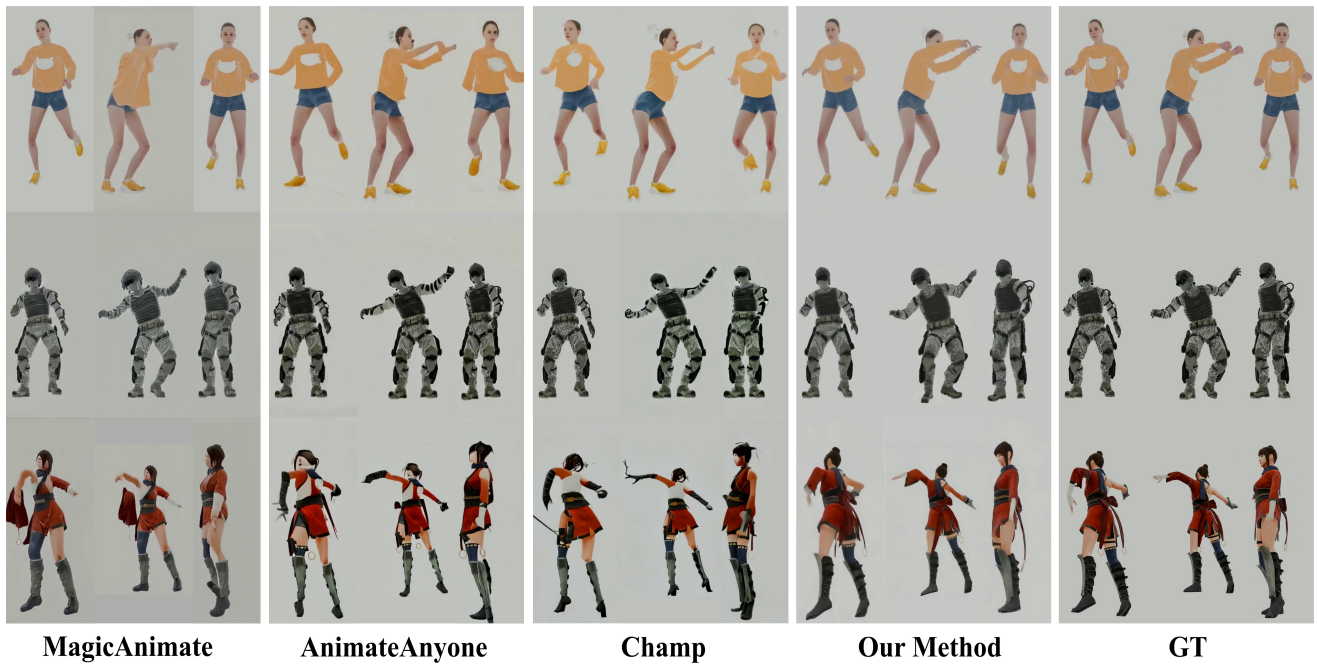


Figure 6. Qualitative comparison free-view video.

egy as the multi-view setting. Quantitative comparisons are presented in Tab. 4. We mask out the backgrounds for a fair comparison since other methods tend to generate noisy backgrounds. Our method outperforms others, demonstrating the 4D diffusion transformer’s ability to learn physical 3D viewpoint changes. We have also conducted qualitative comparisons, with results shown in Fig. 5. Our method generates spatially consistent free-view videos compared to other approaches. Please refer to our submitted project webpage for 3D static video effects.

**Comparisons on Free-view Video.** For free-view video evaluation, we select 10 4D scans from the Human4DiT dataset, each performing 5 different motions, and render them with different camera trajectories to create 50 test videos. We use the frontal view as the reference image. During inference, our method employs the same spatial-temporal sampling strategy as the multi-view setting. Quantitative comparisons are presented in Tab. 5, where we mask out the backgrounds for the evaluation. The results demonstrate our 4D diffusion transformer’s ability to handle both viewpoint and human motion changes in a 4D dynamic scenario. We have also conducted qualitative comparisons, with results shown in Fig. 6. Our method generates spatio-temporally consistent free-viewpoint dynamic videos compared to other approaches. Please refer to our submitted project webpage for free-view video effects.

### 7.3. Ablation Study

To validate the effectiveness of introducing the fourth view dimension and the view transformer in our 4D transformer, we conducted ablation studies for multi-view video, 3D static video, and free-view video generation tasks. Specifically, we disabled the view transformer and relied solely on the temporal transformer to generate the corresponding videos. Quantitative comparisons are presented in Tab. 3, 4, 5. It can be observed that the introduction of the view transformer leads to improvements in view-related generation tasks, demonstrating the efficacy of the view transformer.

## 8. Discussion

**Conclusion.** We have presented a novel method for human video generation, which takes as input only a single image and produces spatio-temporally coherent video of dynamic human motions under free viewpoints. Our approach employs an efficient 4D transformer architecture to model the correlations across multiple domains, including view, time and poses. Combining with UNets for accurate condition injection, our model can be trained on a multi-dimensional dataset spanning images, videos, multi-view data, and 4D scans. After training, our method can synthesize realistic, coherent human motion videos from free viewpoints, and

we believe our contributions will inspire future work towards 4D content generation.

**Limitations.** Instead of generating an explicit 4D models, our method directly synthesizes 2D videos from the given viewpoints, and the 4D scene structure are implicitly encoded through the attention mechanism. The absence of an explicit 4D representation results in some subtle artifacts when rendering free-view videos. Furthermore, our current implementation cannot generate tiny structures coherently, such as fingers and accessories. Future works may incorporate body part-aware generator to resolve this limitation.

## References

- [1] Fan Bao, Shen Nie, Kaiwen Xue, Yue Cao, Chongxuan Li, Hang Su, and Jun Zhu. All are worth words: A vit backbone for diffusion models. In *Proceedings of the IEEE/CVF Conference on Computer Vision and Pattern Recognition*, pages 22669–22679, 2023. 3
- [2] Ankan Kumar Bhunia, Salman Khan, Hisham Cholakkal, Rao Muhammad Anwer, Jorma Laaksonen, Mubarak Shah, and Fahad Shahbaz Khan. Person image synthesis via denoising diffusion model. In *Proceedings of the IEEE/CVF Conference on Computer Vision and Pattern Recognition*, pages 5968–5976, 2023. 3
- [3] Michael J Black, Priyanka Patel, Joachim Tesch, and Jinlong Yang. Bedlam: A synthetic dataset of bodies exhibiting detailed lifelike animated motion. In *Proceedings of the IEEE/CVF Conference on Computer Vision and Pattern Recognition*, pages 8726–8737, 2023. 5
- [4] Wei Cheng, Ruixiang Chen, Siming Fan, Wanqi Yin, Keyu Chen, Zhongang Cai, Jingbo Wang, Yang Gao, Zhengming Yu, Zhengyu Lin, et al. Dna-rendering: A diverse neural actor repository for high-fidelity human-centric rendering. In *Proceedings of the IEEE/CVF International Conference on Computer Vision*, pages 19982–19993, 2023. 5
- [5] Ian Goodfellow, Jean Pouget-Abadie, Mehdi Mirza, Bing Xu, David Warde-Farley, Sherjil Ozair, Aaron Courville, and Yoshua Bengio. Generative adversarial nets. *Advances in neural information processing systems*, 27, 2014. 2
- [6] Hao He, Yinghao Xu, Yuwei Guo, Gordon Wetzstein, Bo Dai, Hongsheng Li, and Ceyuan Yang. Cameractrl: Enabling camera control for text-to-video generation, 2024. 3
- [7] Li Hu, Xin Gao, Peng Zhang, Ke Sun, Bang Zhang, and Liefeng Bo. Animate anyone: Consistent and controllable image-to-video synthesis for character animation. *arXiv preprint arXiv:2311.17117*, 2023. 1, 3, 7
- [8] Yasamin Jafarian and Hyun Soo Park. Learning high fidelity depths of dressed humans by watching social media dance videos. In *Proceedings of the IEEE/CVF Conference on Computer Vision and Pattern Recognition*, pages 12753–12762, 2021. 5
- [9] Xuan Ju, Ailing Zeng, Jianan Wang, Qiang Xu, and Lei Zhang. Human-art: A versatile human-centric dataset bridging natural and artificial scenes. In *Proceedings of the IEEE/CVF Conference on Computer Vision and Pattern Recognition*, pages 618–629, 2023. 5

- [10] Johanna Karras, Aleksander Holynski, Ting-Chun Wang, and Ira Kemelmacher-Shlizerman. Dreampose: Fashion video synthesis with stable diffusion. In *Proceedings of the IEEE/CVF International Conference on Computer Vision*, pages 22680–22690, 2023. 3
- [11] Sunmin Lee, Taeho Kang, Jungnam Park, Jehee Lee, and Jungdam Won. Same: Skeleton-agnostic motion embedding for character animation. In *SIGGRAPH Asia 2023 Conference Papers*, pages 1–11, 2023. 1
- [12] Jing Lin, Ailing Zeng, Shunlin Lu, Yuanhao Cai, Ruimao Zhang, Haoqian Wang, and Lei Zhang. Motion-x: A large-scale 3d expressive whole-body human motion dataset. *Advances in Neural Information Processing Systems*, 36, 2024. 5
- [13] Ruoshi Liu, Rundi Wu, Basile Van Hoorick, Pavel Tokmakov, Sergey Zakharov, and Carl Vondrick. Zero-1-to-3: Zero-shot one image to 3d object. In *Proceedings of the IEEE/CVF International Conference on Computer Vision*, pages 9298–9309, 2023. 3
- [14] Yuan Liu, Cheng Lin, Zijiao Zeng, Xiaoxiao Long, Lingjie Liu, Taku Komura, and Wenping Wang. Syncdreamer: Generating multiview-consistent images from a single-view image. *arXiv preprint arXiv:2309.03453*, 2023. 3
- [15] Xiaoxiao Long, Yuan-Chen Guo, Cheng Lin, Yuan Liu, Zhiyang Dou, Lingjie Liu, Yuexin Ma, Song-Hai Zhang, Marc Habermann, Christian Theobalt, et al. Wonder3d: Single image to 3d using cross-domain diffusion. *arXiv preprint arXiv:2310.15008*, 2023. 3
- [16] Matthew Loper, Naureen Mahmood, Javier Romero, Gerard Pons-Moll, and Michael J Black. Smpl: A skinned multi-person linear model. In *Seminal Graphics Papers: Pushing the Boundaries, Volume 2*, pages 851–866. 2023. 1
- [17] Haoyu Lu, Guoxing Yang, Nanyi Fei, Yuqi Huo, Zhiwu Lu, Ping Luo, and Mingyu Ding. Vdt: General-purpose video diffusion transformers via mask modeling. In *The Twelfth International Conference on Learning Representations*, 2023. 3
- [18] Xin Ma, Yaohui Wang, Gengyun Jia, Xinyuan Chen, Ziwei Liu, Yuan-Fang Li, Cunjian Chen, and Yu Qiao. Latte: Latent diffusion transformer for video generation. *arXiv preprint arXiv:2401.03048*, 2024. 3
- [19] Mehdi Mirza and Simon Osindero. Conditional generative adversarial nets. *arXiv preprint arXiv:1411.1784*, 2014. 2
- [20] OpenAI. Video generation models as world simulators. <https://openai.com/index/video-generation-models-as-world-simulators/>, 2024. Accessed: 2024-05-19. 2, 3
- [21] William Peebles and Saining Xie. Scalable diffusion models with transformers. In *Proceedings of the IEEE/CVF International Conference on Computer Vision*, pages 4195–4205, 2023. 2, 3
- [22] Alec Radford, Karthik Narasimhan, Tim Salimans, Ilya Sutskever, et al. Improving language understanding by generative pre-training. 2018. 3
- [23] Alec Radford, Jeffrey Wu, Rewon Child, David Luan, Dario Amodei, Ilya Sutskever, et al. Language models are unsupervised multitask learners. *OpenAI blog*, 1(8):9, 2019. 3
- [24] Robin Rombach, Andreas Blattmann, Dominik Lorenz, Patrick Esser, and Björn Ommer. High-resolution image synthesis with latent diffusion models. In *Proceedings of the IEEE/CVF conference on computer vision and pattern recognition*, pages 10684–10695, 2022. 1
- [25] Olaf Ronneberger, Philipp Fischer, and Thomas Brox. U-net: Convolutional networks for biomedical image segmentation. In *Medical image computing and computer-assisted intervention—MICCAI 2015: 18th international conference, Munich, Germany, October 5-9, 2015, proceedings, part III 18*, pages 234–241. Springer, 2015. 1, 3
- [26] Ruoxi Shi, Hansheng Chen, Zhuoyang Zhang, Minghua Liu, Chao Xu, Xinyue Wei, Linghao Chen, Chong Zeng, and Hao Su. Zero123++: a single image to consistent multi-view diffusion base model. *arXiv preprint arXiv:2310.15110*, 2023. 3
- [27] Yichun Shi, Peng Wang, Jianglong Ye, Mai Long, Kejie Li, and Xiao Yang. Mvdream: Multi-view diffusion for 3d generation. *arXiv preprint arXiv:2308.16512*, 2023. 3
- [28] Aliaksandr Siarohin, Enver Sangineto, Stéphane Lathuilière, and Nicu Sebe. Deformable gans for pose-based human image generation. In *Proceedings of the IEEE conference on computer vision and pattern recognition*, pages 3408–3416, 2018. 2
- [29] Aliaksandr Siarohin, Stéphane Lathuilière, Enver Sangineto, and Nicu Sebe. Appearance and pose-conditioned human image generation using deformable gans. *IEEE transactions on pattern analysis and machine intelligence*, 43(4):1156–1171, 2019.
- [30] Aliaksandr Siarohin, Stéphane Lathuilière, Sergey Tulyakov, Elisa Ricci, and Nicu Sebe. First order motion model for image animation. *Advances in neural information processing systems*, 32, 2019. 2
- [31] Robin Strudel, Ricardo Garcia, Ivan Laptev, and Cordelia Schmid. Segmenter: Transformer for semantic segmentation. In *Proceedings of the IEEE/CVF international conference on computer vision*, pages 7262–7272, 2021. 3
- [32] Yu Tian, Jian Ren, Menglei Chai, Kyle Olszewski, Xi Peng, Dimitris N Metaxas, and Sergey Tulyakov. A good image generator is what you need for high-resolution video synthesis. *arXiv preprint arXiv:2104.15069*, 2021. 2
- [33] Hugo Touvron, Matthieu Cord, Matthijs Douze, Francisco Massa, Alexandre Sablayrolles, and Hervé Jégou. Training data-efficient image transformers & distillation through attention. In *International conference on machine learning*, pages 10347–10357. PMLR, 2021. 3
- [34] Shuhei Tsuchida, Satoru Fukayama, Masahiro Hamasaki, and Masataka Goto. Aist dance video database: Multi-genre, multi-dancer, and multi-camera database for dance information processing. In *Proceedings of the 20th International Society for Music Information Retrieval Conference, ISMIR 2019, Delft, Netherlands, 2019*. 5
- [35] Twindom. Twindom 3d avatar dataset, 2022. 5
- [36] Ashish Vaswani, Noam Shazeer, Niki Parmar, Jakob Uszkoreit, Llion Jones, Aidan N Gomez, Łukasz Kaiser, and Illia Polosukhin. Attention is all you need. *Advances in neural information processing systems*, 30, 2017. 3

- [37] Tan Wang, Linjie Li, Kevin Lin, Chung-Ching Lin, Zhengyuan Yang, Hanwang Zhang, Zicheng Liu, and Lijuan Wang. Disco: Disentangled control for referring human dance generation in real world. *arXiv e-prints*, pages arXiv-2307, 2023. 1, 3, 7
- [38] Ting-Chun Wang, Arun Mallya, and Ming-Yu Liu. One-shot free-view neural talking-head synthesis for video conferencing. In *Proceedings of the IEEE/CVF conference on computer vision and pattern recognition*, pages 10039–10049, 2021. 2
- [39] Yaohui Wang, Piotr Bilinski, Francois Bremond, and Antitza Dantcheva. G3an: Disentangling appearance and motion for video generation. In *Proceedings of the IEEE/CVF Conference on Computer Vision and Pattern Recognition*, pages 5264–5273, 2020. 2
- [40] Enze Xie, Wenhai Wang, Zhiding Yu, Anima Anandkumar, Jose M Alvarez, and Ping Luo. Segformer: Simple and efficient design for semantic segmentation with transformers. *Advances in neural information processing systems*, 34: 12077–12090, 2021. 3
- [41] Zhongcong Xu, Jianfeng Zhang, Jun Hao Liew, Hanshu Yan, Jia-Wei Liu, Chenxu Zhang, Jiashi Feng, and Mike Zheng Shou. Magicanimate: Temporally consistent human image animation using diffusion model. *arXiv preprint arXiv:2311.16498*, 2023. 1, 3, 7
- [42] Shiyuan Yang, Liang Hou, Haibin Huang, Chongyang Ma, Pengfei Wan, Di Zhang, Xiaodong Chen, and Jing Liao. Direct-a-video: Customized video generation with user-directed camera movement and object motion. *arXiv preprint arXiv:2402.03162*, 2024. 3
- [43] Hongwei Yi, Hualin Liang, Yifei Liu, Qiong Cao, Yandong Wen, Timo Bolkart, Dacheng Tao, and Michael J Black. Generating holistic 3d human motion from speech. In *IEEE Conference on Computer Vision and Pattern Recognition (CVPR)*, pages 469–480, 2023. 5
- [44] Tao Yu, Zerong Zheng, Kaiwen Guo, Pengpeng Liu, Qionghai Dai, and Yebin Liu. Function4d: Real-time human volumetric capture from very sparse consumer rgbd sensors. In *IEEE Conference on Computer Vision and Pattern Recognition (CVPR2021)*, 2021. 5
- [45] Li Yuan, Yunpeng Chen, Tao Wang, Weihao Yu, Yujun Shi, Zi-Hang Jiang, Francis EH Tay, Jiashi Feng, and Shuicheng Yan. Tokens-to-token vit: Training vision transformers from scratch on imagenet. In *Proceedings of the IEEE/CVF international conference on computer vision*, pages 558–567, 2021. 3
- [46] Hongwen Zhang, Siyou Lin, Ruizhi Shao, Yuxiang Zhang, Zerong Zheng, Han Huang, Yandong Guo, and Yebin Liu. Closet: Modeling clothed humans on continuous surface with explicit template decomposition. In *Proceedings of the IEEE/CVF Conference on Computer Vision and Pattern Recognition*, pages 501–511, 2023. 5
- [47] Lvmin Zhang, Anyi Rao, and Maneesh Agrawala. Adding conditional control to text-to-image diffusion models. In *Proceedings of the IEEE/CVF International Conference on Computer Vision*, pages 3836–3847, 2023. 1
- [48] Hongkai Zheng, Weili Nie, Arash Vahdat, and Anima Anandkumar. Fast training of diffusion models with masked transformers. *arXiv preprint arXiv:2306.09305*, 2023. 3
- [49] Sixiao Zheng, Jiachen Lu, Hengshuang Zhao, Xiatian Zhu, Zekun Luo, Yabiao Wang, Yanwei Fu, Jianfeng Feng, Tao Xiang, Philip HS Torr, et al. Rethinking semantic segmentation from a sequence-to-sequence perspective with transformers. In *Proceedings of the IEEE/CVF conference on computer vision and pattern recognition*, pages 6881–6890, 2021. 3
- [50] Shenao Zhu, Junming Leo Chen, Zuozhuo Dai, Yinghui Xu, Xun Cao, Yao Yao, Hao Zhu, and Siyu Zhu. Champ: Controllable and consistent human animation with 3d parametric guidance. *arXiv preprint arXiv:2403.14781*, 2024. 1, 3, 7